Available online at www.sciencedirect.com
ScienceDirect
Cellular Signalling 19 (2007) 1446–1456
CELLULAR SIGNALLING
www.elsevier.com/locate/cellsig

The activation mechanism of chemokine receptor CCR5 involves common structural changes but a different network of interhelical interactions relative to rhodopsin

Jean-Yves Springael [a,1], Cédric de Poorter [a,1], Xavier Deupi [b], Joost Van Durme [a], Leonardo Pardo [b], Marc Parmentier [a,*]

[a] Institut de Recherche Interdisciplinaire en Biologie Humaine et Moléculaire (IRIBHM), ULB Campus Erasme, 808 Route de Lennik, B-1070 Brussels, Belgium
[b] Laboratori de Medicina Computacional, Unitat de Bioestadística, Universitat Autònoma de Barcelona, 08193 Bellaterra, Spain

Received 3 January 2007; received in revised form 15 January 2007; accepted 15 January 2007
Available online 25 January 2007

Abstract

In G protein-coupled receptors (GPCRs), the interaction between the cytosolic ends of transmembrane helix 3 (TM3) and TM6 was shown to play an important role in the transition from inactive to active states. According to the currently prevailing model, constructed for rhodopsin and structurally related receptors, the arginine of the conserved "DRY" motif located at the cytosolic end of TM3 (R3.50) would interact with acidic residues in TM3 (D/E3.49) and TM6 (D/E6.30) at the resting state and shift out of this polar pocket upon agonist stimulation. However, 30% of GPCRs, including all chemokine receptors, contain a positively charged residue at position 6.30 which does not support an interaction with R3.50. We have investigated the role of R6.30 in this receptor family by using CCR5 as a model. R6.30D and R6.30E substitutions, which allow an ionic interaction with R3.50, resulted in an almost silent receptor devoid of constitutive activity and strongly impaired in its ability to bind chemokines but still able to internalize. R6.30A and R6.30Q substitutions, allowing weaker interactions with R3.50, preserved chemokine binding but reduced the constitutive activity and the functional response to chemokines. These results indicate that the constitutive and ligand-promoted activity of CCR5 can be modified by modulating the interaction between the DRY motif in TM3 and residues in TM6 suggesting that the overall structure and activation mechanism are well conserved in GPCRs. However, the molecular interactions locking the inactive state must be different in receptors devoid of D/E6.30.

Keywords: Activation; CCR5; Constitutive activity

1. Introduction

The CC chemokine receptor CCR5 is expressed on memory T lymphocytes and the monocyte-macrophage lineage [1–3] and responds to nanomolar concentrations of MIP-1α/CCL3, MIP-1β/CCL4, RANTES/CCL5, MCP-2/CCL8 and a truncated form of HCC-1/CCL14 [4–6]. When expressed in recombinant systems, CCR5 displays a constitutive activity that is inhibited by inverse agonists such as TAK-779 [7]. The physiological significance of this constitutive activity in vivo remains however to be determined. In addition to its role as a chemokine receptor involved in the recruitment of leukocytes in a number of physiological and pathological situations (such as rheumatoid arthritis, graft rejection, neurodegenerative diseases and asthma), CCR5 constitutes the major co-receptor for macrophage-tropic strains of human immunodeficiency virus (HIV). It allows, together with CD4, the binding of the viral particles to the cell surface through the envelope protein gp120, and this interaction triggers the subsequent membrane fusion process [8,9]. CCR5 forms homodimers, but also heterodimers with its closest homologue CCR2, in a ligand-independent manner [10–16]. This oligomeric organization was demonstrated in native cells, and has functional consequences, as negative binding cooperativity was demonstrated between the binding pockets of each protomer, resulting in the binding of a single chemokine molecule per receptor dimer [15,16].

* Corresponding author. Tel.: +32 2 555 41 71; fax: +32 2 555 46 55.
E-mail address: mparment@ulb.ac.be (M. Parmentier).
[1] These two authors contributed equally to this work.

0898-6568/$ - see front matter © 2007 Elsevier Inc. All rights reserved.
doi:10.1016/j.cellsig.2007.01.022

In the absence of experimentally determined tridimensional structures for any other member of the GPCR family,[17] the bovine rhodopsin crystal structure is used as a template for homology modeling of rhodopsin-like GPCRs and as a common support for structure–function relationship studies [18]. Biochemical and biophysical approaches, supported by modeling studies, have identified key structural motifs involved in the activation mechanism of GPCRs [19–22]. Labeling of receptors with fluorescent probes sensitive to the changes in biophysical environment provided evidence that activation of selected GPCRs involved relative movements of their TM3 and TM6, suggesting that the activation mechanisms would require the disruption of intramolecular interactions that stabilize the receptor in its inactive conformation [23]. One such constrain is the ionic lock between the arginine of the highly conserved (D/E)RY motif in TM3 with its adjacent Asp/Glu residue and an Asp/Glu residue at the cytoplasmic end of TM6, which is conserved in a large subset of GPCRs [24]. Disruption of these constrains can be promoted either by agonists or by mutations affecting the key residues involved and it has been demonstrated that charge-neutralizing mutations of D3.49 or R3.50 in TM3, and D/E6.30 in TM6, results in increased constitutive activity of rhodopsin and a number of structurally-related class A GPCRs [19,25–29]. However, these charged residues are not shared by all GPCRs and different interactions might therefore regulate the equilibrium between inactive and active states in some receptor subfamilies, more distantly related to rhodopsin. Among these, chemokine receptors in general and CCR5 in particular do not share with rhodopsin the negatively charged residue at position 6.30, which is occupied by an arginine. It was also shown previously that mutation of D3.49, within the "DRY box" of CCR5, results in a reduction, rather than an increase, of both the basal and agonist-induced activity of the receptor [7]. We have now extended this study by investigating more specifically the role of the R6.30 residue located at the cytosolic end of TM6. The nature of this amino acid does not allow an ionic interaction with the R3.50 of TM3 and the locking of CCR5 in an inactive state. In addition, chemokine receptors contain also the family-conserved D2.40 in TM2, which is Asn in rhodopsin and in most other members of class A GPCRs. It was shown that mutation of D2.40 increased the constitutive activity of the chemokine-homologous Kaposi's sarcoma-associated herpesvirus GPCR [30]. In order to study the role of these chemokine family-specific residues we replaced by using site-directed mutagenesis R6.30 and D2.40 with various amino-acids to modulate their potential inter-helical interactions and analyzed the properties of the resulting mutants in terms of cell surface expression, receptor dimerization, chemokine binding, basal and chemokine-stimulated activity and receptor internalization.

2. Experimental procedures

2.1. Numbering scheme of GPCRs

We use in this work a general numbering scheme identifying residues located at the same position in the transmembrane segments of different receptors [31]. Each residue is numbered according to the helix (1 through 7) in which it is located and to the position relative to the most conserved residue in that helix, arbitrarily assigned to 50. For instance, R6.30 is the arginine in transmembrane helix 6 (TM6) twenty residues before the highly conserved proline P6.50.

2.2. Construction of CCR5 mutants

Plasmids encoding the CCR5 mutants were constructed by site-directed mutagenesis using the QuikChange method (Stratagene). Following sequencing of the constructs, the mutated coding sequences were subcloned into the bicistronic expression vector pEFIN3, as previously described, for the generation of stable cell lines [32]. All constructs were verified by sequencing prior to transfection.

2.3. Expression of mutant receptors in CHO-K1 Cells

CHO-K1 cells were cultured in Ham's F-12 medium supplemented with 10% fetal calf serum (Invitrogen), 100 units/ml of penicillin and 100 μg/ml of streptomycin (Invitrogen). Constructs encoding wild-type or mutant CCR5 in the pEFIN3 vector were transfected using FusGENE 6 (Roche Molecular Biochemicals) in a CHO-K1 cell line expressing an apoaequorin variant targeted to mitochondria. Selection of transfected cells was made for 14 days with 400 μg/ml G418 (Invitrogen) and 250 μg/ml zeocin (Invitrogen, for maintenance of the apoaequorin encoding plasmid) and the population of mixed cell clones expressing wild-type or mutant receptors was used for binding and functional studies. Cell surface expression of the receptor variants was measured by flow cytometry using monoclonal antibodies recognizing different CCR5 epitopes: 2D7 (phycoerythrin-conjugated, PharMingen) or MC-5 (kindly provided by Mathias Mack, Munich, Germany). Unlabeled monoclonal antibodies were detected by a phycoerythrin-coupled anti-mouse IgG secondary antibody (Sigma).

2.3.1. GTPγS binding assay

Membranes (10–20 μg) of cells expressing CCR5 were incubated for 15 min at room temperature in binding buffer (20 mM HEPES, pH 7.4, 100 mM NaCl, 3 mM $MgCl_2$, 3 μM GDP, 10 μg/ml saponine) containing chemokines or mAbs in 96-well microplates (Basic Flashplates, PerkinElmer Life Sciences). GTPγ^{35}S (0.1 nM, Amersham) was added and microplates were incubated for 30 min at 30 °C in the absence or presence of 1 μM TAK-779. Incubation was stopped by centrifugation of the microplates for 10 min at 800 g and 4 °C, followed by supernatant removal. Microplates were counted in a TopCount (Packard Instrument Co.) for 1 min per well.

2.3.2. Binding assay

Cells expressing receptors were grown near to confluence, collected from plates in Ca^{2+}- and Mg^{2+}-free PBS, centrifuged for 5 min at 1500 g and washed with PBS. Cells were then resuspended in buffer A (15 mM Tris–HCl pH 7.5, 2 mM $MgCl_2$, 0.3 mM EDTA, 1 mM EGTA) and disrupted in a glass homogenizer. The homogenates were first centrifuged for 5 min at 500 *g* and the resulting supernatants at 40,000 *g* for 30 min at 4 °C. The cell membrane pellet was washed in buffer A, and resuspended in buffer B (75 mM Tris–HCl pH 7.5, 12.5 mM $MgCl_2$, 0.3 mM EDTA, 1 mM EGTA, 250 mM sucrose) at a protein concentration of approximately 1 mg/ml. Competition binding experiments were performed by using 0.2 nM ^{125}I-MIP-1β as labeled tracer and variable concentrations of chemokines as unlabeled competitors. Samples were incubated for 60 min at 27 °C, and then bound tracer was separated by filtration through GF/B filters presoaked in 0.5% BSA. Filters were counted in a γ-scintillation counter. Binding parameters were determined with the PRISM software (Graphpad Softwares) using nonlinear regression applied to a single site binding model.

2.4. Aequorin-based functional assay

The functional response to chemokines was estimated by an aequorin-based assay [5]. Briefly, cells were harvested from plates with Ca^{2+}- and Mg^{2+}-free DMEM supplemented with 5 mM EDTA and centrifuged for 2 min at 1000 *g*. The pellet was resuspended in DMEM at a density of 5×10^6 cells/ml, and incubated for 4 h in the dark in the presence of 5 μM coelenterazine H (Promega Corporation). Cells were then diluted 5-fold before use. Variable concentrations of chemokines in a volume of 50 μl of DMEM were added to 50 μl of cell suspension (25,000 cells) per well. Luminescence was measured for 30 s in an EG and G Berthold luminometer (PerkinElmer Life Sciences). Half-maximal effective concentrations

(EC_{50}) were determined with the GraphPad Prism software using nonlinear regression applied to a sigmoidal dose-response model. The reported values are the mean ± S.E.M. of at least three independent experiments.

2.5. Phosphorylated p42/p44 MAP-kinase assay

Cells were serum-starved for 24 h and resuspended in 37 °C pre-warmed serum-free DMEM one hour before stimulation. After 3 min of stimulation with various concentrations of MIP-1β, cells were collected by centrifugation and heated to 100 °C for 5 min in lysis buffer (100 mM Tris-HCl, pH 6.8, 4 mM EDTA, 4% SDS, 20% glycerol, and 0.02% β-mercaptoethanol). For Western blot analysis, solubilized proteins corresponding to 5×10^5 cells were loaded onto 10% SDS-polyacrylamide gels in a Tricine buffer system. After transfer to nitrocellulose membranes, proteins were probed with mouse anti-phospho-p42/p44 (1:1000) or rabbit anti-total-p42/p44 (1:2000) antibodies (Cell Signaling Technology). Immobilized antigen–antibody complexes were detected with secondary horseradish peroxidase conjugated anti-species-IgG-(Amersham), developed by enhanced chemiluminescence (ECL+, Amersham).

2.6. Receptor down-modulation assay

Cells were serum-starved for 12 h and incubated at 37 °C for 30 min in DMEM in the presence or absence of CCL4 at various concentrations. Once treated, cells were placed on ice and then washed twice with ice-cold PBS. To remove receptor-bound CCL4, cells were incubated for 2 min in 50 mM glycine, pH 2.7, containing 100 mM NaCl, and subsequently diluted up to 1 ml with ice-cold PBS/0.1% BSA/0.1% NaN_3 buffer. Cells were washed twice with the same buffer before staining with PE-conjugated 2D7 mAb and analysis by flow cytometry. No receptor down-modulation was found when cells were incubated at 4 °C in the presence of ligand.

2.7. BRET assay

The cDNAs encoding EYFP and a humanized form of *Renilla* luciferase were fused in frame to the 3′ end of CCR5 in the pcDNA3.1 vector, as described previously [12]. A BRET protocol adapted to cell monolayers was developed and the BRET experiments performed as described [20,33]. Human embryonic kidney (HEK-293T) cells were transfected by the calcium phosphate precipitation method with different receptor combinations. A control corresponding to mock-transfected cells was included in order to subtract the raw basal luminescence. Forty-eight hours after transfection, the BRET measurement was performed using a Mithras LB 940 Multilabel Reader (Berthold) as described [15,20]. The BRET ratio is defined as [(emission at 510–590)/(emission at 440–500)] − *Cf* where *Cf* corresponds to (emission at 510–590)/(emission at 440–500) for the *-hRluc* construct expressed alone in the same experiment.

2.8. Molecular modeling

The previously reported molecular model of CCR5 was used throughout this manuscript [34,35]. This model takes into account the presence of the T2.56-X-P2.58 motif in TM2 that results in the bending of its extracellular moiety toward TM3 [36] and the subsequent relocation of TM3 toward TM5 [35]. Water molecules 1, 2, 7, 9, and 12 observed in the P6.50/D2.50/N7.49/Y7.53 environment of rhodopsin were also included in the model [37]. These structural water molecules mediate a number of interhelical interactions that are important in maintaining the inactive state of the receptor [20,21]. Several procedures have been described for measuring the distortion of transmembrane α-helices [38,39]. We will refer in this manuscript to two relevant parameters. First, the bend angle, defined as the angle between the axis of the cylinders formed by the residues preceding and following the motif that induces the distortion in the helix. Second, a residue-residue twist angle, or unit twist, calculated for sets of four consecutive Cα atoms, i.e. one turn, to analyze helical uniformity [38]. An ideal α-helix, with approximately 3.6 residues per turn, has a unit twist of approximately 100° (360°/3.6). A closed helical segment, with <3.6 residues per turn, possesses a unit twist >100°, whereas an open helical segment, with >3.6 residues per turn, possesses a unit twist <100°. Correlation between the physico-chemical properties of the side chains at various positions were obtained with the Alignment Explorer Software available at the GRIS database http://gris.ulb.ac.be [40].

3. Results

3.1. Computational analysis of TM 6 and its environment in rhodopsin and chemokine receptors

In rhodopsin, TM6 displays a bend angle of 35°, which is much higher than the average 20° bend angle of Pro-kinked α-helices, and is opened by 20° at the 6.46–6.49 turn (>3.6 residues/turn, twist of 79°) (Fig. 1A) [37,41,42]. This extreme conformation of TM6, in which both the bend and the twist angles are modified, is energetically stabilized through two structural and functional elements. First, a discrete water molecule in the vicinity of P6.50 of the highly conserved WxP(Y/F) motif stabilizes this unusual Pro-kink conformation. Opening of the helix at the 6.46–

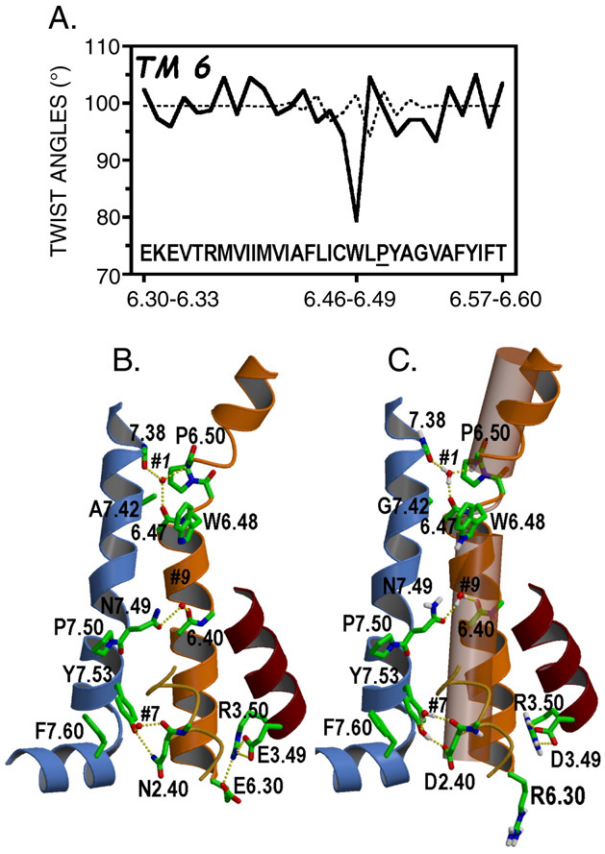

Fig. 1. A. Evolution of the unit twist angles (°) of a standard Pro-kink helix (dashed line) and TM6 of bovine rhodopsin (solid line). The amino acid sequence of TM6 in rhodopsin is shown (P6.50 is underlined). (B, C) Detailed view of the network of interactions involving highly conserved amino-acids within TMs 2, 6, and 7 and Hx8 in rhodopsin (PDB code 1GZM) (B) and a rhodopsin-based CCR5 model C. The strong distortion at P6.50 is partly stabilized by water#1, which links the backbone carbonyl at position 6.47 with the backbone N–H amide at position 6.51. Water#9 mediates an inter-helical interaction between the side chain of N7.49 and the backbone carbonyl at position 6.40 to maintain the receptor in the inactive state. Water#7 participates in a network of interactions between Y7.53 with N2.40 in rhodopsin or D2.40 in CCR5 and FY.53. The ionic lock linking the intracellular part of TM3 and TM6 in rhodopsin is absent in CCR5 due to the presence of R6.30 instead of E6.30. The α-carbon ribbons of TM2 (goldenrod), TM3 (dark red), TM6 (orange) and TM7 (blue) are displayed. A standard Pro-kink α-helix (depicted as a cylinder) is superimposed onto the backbones of the WxP(F/Y) motif and residue 6.40 of TM6 in the CCR5 model.

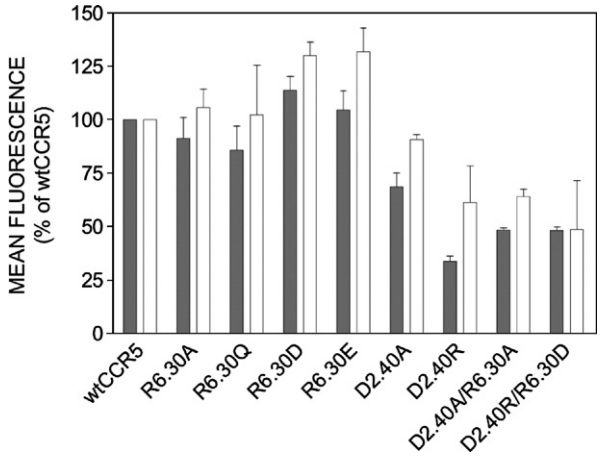

Fig. 2. Cell surface expression of CCR5 mutants. Cell surface expression of wt or mutant forms of CCR5 was measured by fluorescence-activated cell sorting using 2 different monoclonal antibodies. The 2D7 antibody (open bars) recognizes a conformational epitope centered on ECL2, whereas MC-5 (filled bars) targets a linear epitope located in the N-terminal domain of CCR5. Values represent the average of mean cell fluorescence derived from three independent experiments (error bar indicate S.E.M.).

6.49 turn disrupts the intra-helical hydrogen bond between the carbonyl group at position 6.47 and the N–H amide at positions 6.51 (Fig. 1B). Wat#1 acts as a hydrogen bond acceptor in the interaction with the backbone N–H amide at position 6.51, and as a hydrogen bond donor in the interactions with the backbone carbonyls at positions 6.47 and 7.38 [37]. Importantly, 60% of Class A GPCRs contain a non-bulky aminoacid at position 7.42 (A:40%; G:20%), creating a small cavity between TM6 and TM7 that allows accommodation of this water molecule [43]. The fact that chemokine receptors possess W6.48, involved in the process of receptor activation as shown in the structure of metarhodopsin I [17,22,44], P6.50, and the non-bulky Ala or Gly at position 7.42 suggest that the interface between TMs 6 and 7 at the extracellular domain is similar to rhodopsin (Fig. 1C). The second element that stabilizes the strong bend of TM6 is the ionic and polar interaction of E6.30 and T6.34 with R3.50 of the (D/E)RY motif in TM3 (Fig. 1B) [19,45]. Disruption of this ionic lock induces large conformational changes of TM3 and TM6, considered to be an essential step in the process of GPCR activation [23]. In contrast to the highly conserved (D/E)RY motif in TM3, the acidic residue at position 6.30 is only present in 32% of GPCRs [46,47]. Opioid receptors feature a Leu in 6.30, and the role of E6.30 in rhodopsin is likely to be played by T6.34 in opioid receptors, through a similar although specific set of intramolecular interactions with R3.50 [45]. Chemokine receptors, as well as about 34% of class A GPCRs, contain a basic residue at position 6.30 (K: 18%, R: 16%) [46]. As the presence of a positively charged residue at that position is incompatible with an interaction with the R3.50 of TM3, the network of TM3–TM6 interhelical interactions in these receptors is likely different from that determined in rhodopsin (Fig. 1C, see discussion). Thus, we aim to explore the putative role of the positive side chain at position 6.30 in CCR5.

Another important element in the process of GPCR activation is the highly conserved NPxxY motif in TM7. N7.49 acts as an on/off switch by adopting two different conformations in the inactive and active states [20]. N7.49 is restrained in the inactive state, in rhodopsin and possibly most other GPCRs, towards TM 6 by water#9, which mediates an inter-helical interaction between

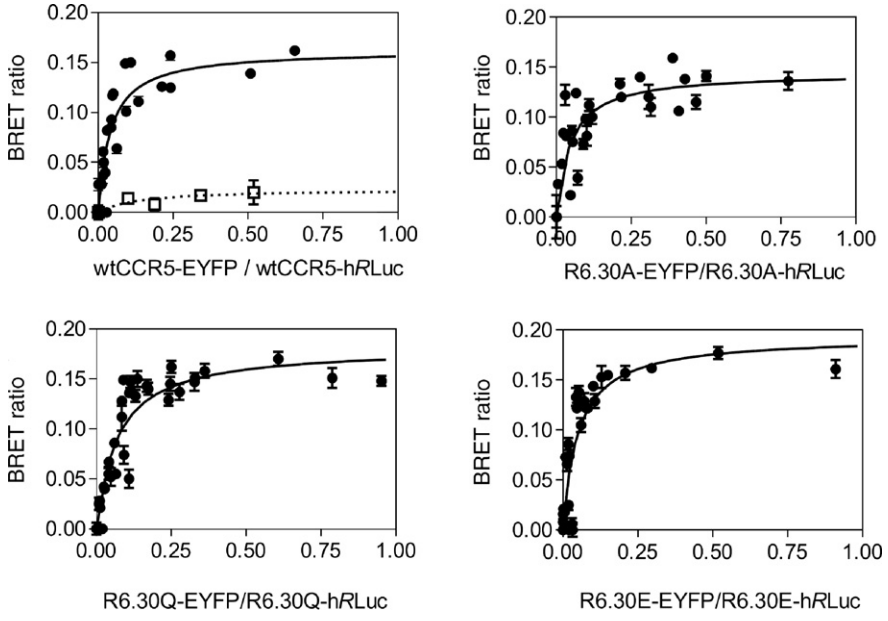

Fig. 3. Oligomerization of CCR5 mutants. HEK-293T cells were transfected with a constant amount of the wt or mutant CCR5-h*R*Luc fusion and increasing amounts of the corresponding EYFP fusion. Dimerization of CCR5 was investigated by measuring the energy transfer between the two partners at room temperature. The graph represents the BRET ratio (see Experimental procedures) over the relative level of expression of CCR5-EYFP and CCR5-h*R*Luc. The analysis was performed using GraphPad Prism software v4.0 using nonlinear regression assuming a single-site saturation binding model. This figure is the compilation of three independent experiments carried out with triplicate data points (error bars indicate S.E.M.). Open squares in the upper left panel represent the transfer of energy between CCR5-h*R*Luc and GABAbR2-EYFP used as a control of specificity.

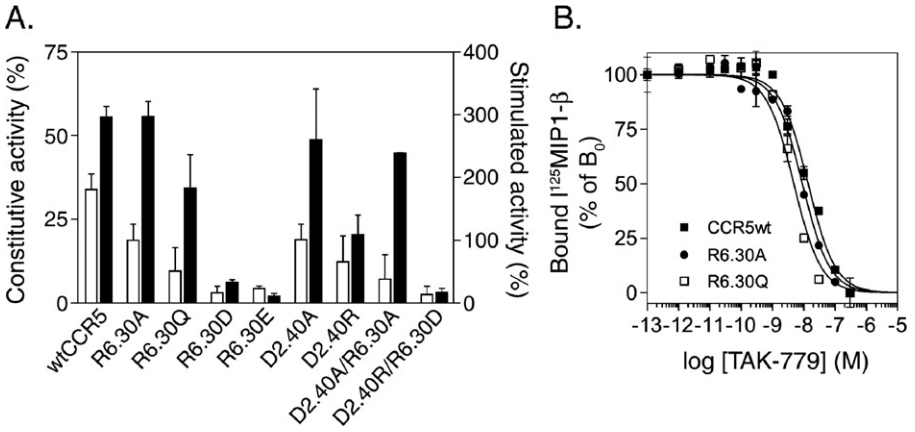

Fig. 4. Constitutive activity of CCR5 mutants. A. GTP-γ^{35}S binding to membranes from CHO-K1 cells expressing wtCCR5 or CCR5 mutants. Constitutive activity (white bars, left scale) corresponds to the value of bound GTP-γ^{35}S in buffer alone (100%) minus de value in the presence of TAK-779. Stimulated activity (black bars, right scale) corresponds to the value of bound GTP-γ^{35}S in presence of 50 nM RANTES reported minus the value of bound GTP-γ^{35}S in buffer alone (100%). The data represent the mean of five independent experiments, each carried out with triplicate data points (error bars indicate S.E.M.). B. Competition binding assays were performed on CHO-K1 cells expressing wt or mutant CCR5, using ^{125}I-MIP-1β as tracer and TAK-779 as competitor. The data were normalized for nonspecific binding, determined in the presence of 300 nM MIP-1β (0%), and specific binding in the absence of competitor (100%). The displayed data are representative of at least three independent experiments. All data points were performed in triplicates (error bars indicate S.E.M.).

the side chain of N7.49 and the backbone carbonyl at position 6.40 (Fig. 1B) [48]. In addition, Y7.53 interacts with F7.60 in Hx8 and with the side chain and backbone (via water molecule #7) of N2.40 in TM2 (Fig. 1B). The Y7.53–F7.60 aromatic–aromatic interaction is disrupted during receptor activation, leading to a proper realigning of Hx8 [49,50]. The conservation pattern of these amino-acids in the chemokine family and the rhodopsin-family of GPCRs suggest a conserved mechanism. However, chemokine receptors contain D2.40 as a substitute to the most common N2.40 (see Fig. 1B and C). It was shown that co-substitution of D2.40 by Ala and V3.49 by Asp, restoring the DRY box, act synergistically to increase basal signaling in the

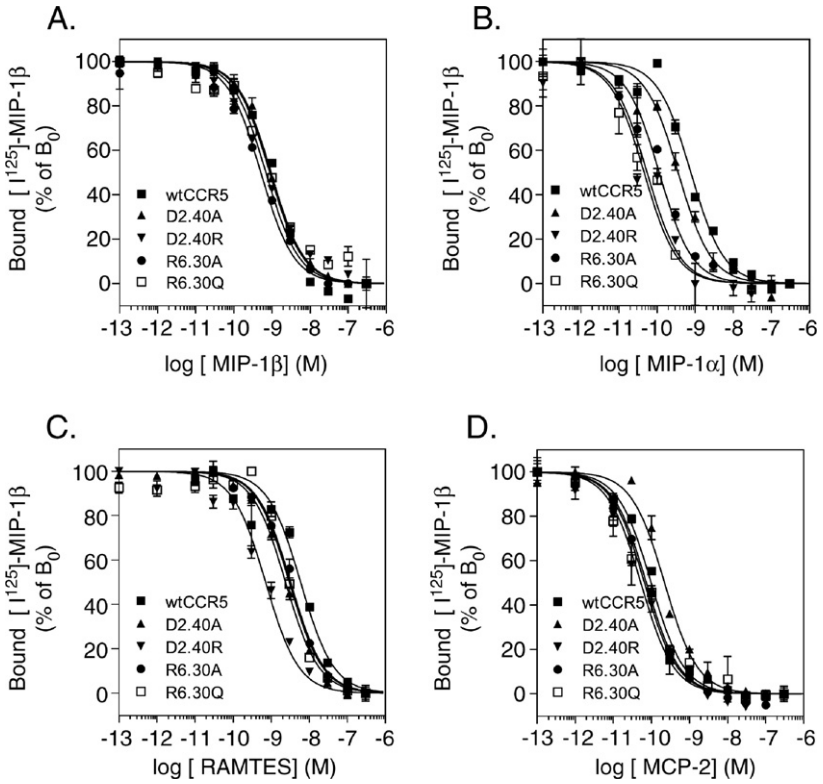

Fig. 5. Ligand binding properties of CCR5 mutants. Competition binding assays were performed on CHO-K1 cells expressing CCR5, using ^{125}I-MIP-1β as tracer, and MIP-1α, MIP-1β, RANTES and MCP-2 as competitors. The data were normalized for nonspecific binding, determined in the presence of 300 nM MIP-1β (0%), and specific binding in the absence of competitor (100%). The displayed data are representative of at least three independent experiments. All data points were performed in triplicates (error bars indicate S.E.M.). No detectable binding was obtained for the R6.30D and R6.30E mutants (not shown).

Table 1
Binding and functional properties of WT and mutant CCR5 receptor

	MIP-1α		MIP-1β		RANTES		MCP-2	
	EC_{50} (nM)	IC_{50} (nM)	EC_{50} (nM)	IC_{50} (nM)	EC_{50} (nM)	IC_{50} (nM)	EC_{50} (nM)	IC_{50} (nM)
CCR5wt	1.08±0.65	0.40±0.34	1.69±0.84	1.07±0.53	2.38±1.71	8.4±0.6	4.28±2.97	0.19±0.1
$R^{6.30}A$	2.99±1.49	0.13±0.04	4.26±2.00	0.59±0.37	15.10±6.12	4.58±1.67	20.21±5.01	0.14±0.07
$R^{6.30}Q$	*N.D.*[a]	0.13±0.08	12.36±5.62	0.64±0.2	34.77±17.45	3.29±0.42	67.75±16.64	0.07±0.02
$D^{2.40}A$	2.80±1.89	0.36±0.12	1.25±0.31	0.57±0.33	1.39±1.72	3.47±1.56	5.12±0.95	0.17±0.09
$D^{2.40}R$	15.65±8.07	0.05±0.01	4.68±1.44	0.34±0.31	9.25±6.57	1.21±0.65	39.39±8.64	0.05±0.01
$D^{2.40}A/R^{6.30}A$	6.95±3.44	*N.T.*[b]	5.08±2.05	*N.T.*[b]	5.03±2.45	*N.T.*[b]	10.40±0.08	*N.T*[b]

The IC_{50} values were obtained from competition binding experiment using ^{125}I-MIP-1β as tracer (as displayed in Fig. 5). The EC_{50} values were obtained from functional dose-response curves using the aequorin assay (as displayed in Fig. 6). Values represent the mean±S.E.M. of at least three independent experiments.
[a] N.D.: not detectable.
[b] N.T.: not tested.

chemokine-homologous Kaposi's sarcoma-associated herpesvirus GPCR [30]. Thus, we also explored in this manuscript the possibility of a relation between the family-specific negatively charged D2.40 and positively charged K/R6.30 amino-acids.

We engineered mutants in which the positively charged arginine 6.30 was substituted by either alanine (R6.30A), aspartate (R6.30D), glutamate (R6.30E), or glutamine (R6.30Q); and the negatively charged aspartate 2.40 was replaced by either alanine (D2.40A), or arginine (D2.40R). We also combined some of these point mutations to generate D2.40A/R6.30A and D2.40R/R6.30D double mutants, with the aim of assessing their additive effects; or rather their compensatory consequences on the receptor function.

3.2. Cells surface expression of the mutant receptors

We first examined the expression of CCR5 mutants at the cell surface by using two well characterized monoclonal antibodies that recognize either a linear epitope at the N-teminus of the receptor (MC-5) or a conformational epitope within the second extracellular loop (2D7) (Fig. 2). The average fluorescence observed in FACS revealed that the R6.30A, R6.30D, R6.30E,

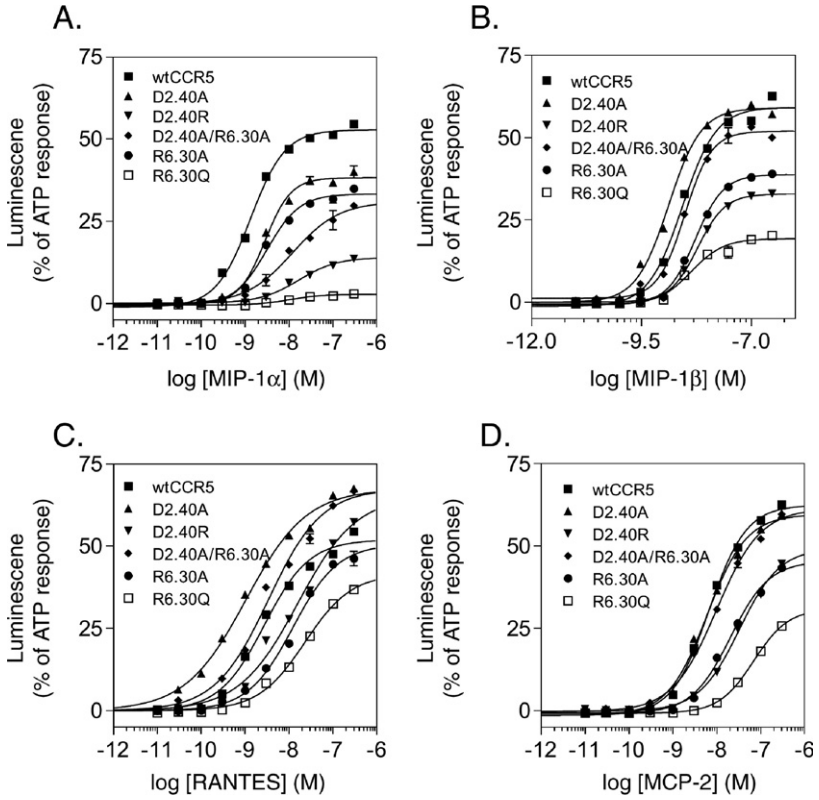

Fig. 6. Functional response of CCR5 mutants. Functional responses of receptors were measured using the aequorin-based functional assay. Cells were incubated with a range of concentrations of MIP-1β, MIP1α, RANTES or MCP-2 and luminescence was recorded for 30 s. The results were normalized for the basal luminescence of the cells in absence of agonist (0%) and the maximal response obtained for each receptor with the 10 μM ATP (100%). The functional parameters (EC_{50}, E_{max}) were determined by nonlinear regression using the GraphPad Prism software and a sigmoidal dose-response model. The displayed data are representative of three independent experiments. All data points were performed in duplicates (error bars indicate S.E.M). No functional response was obtained for the R6.30D and R6.30E mutants in this assay (not shown).

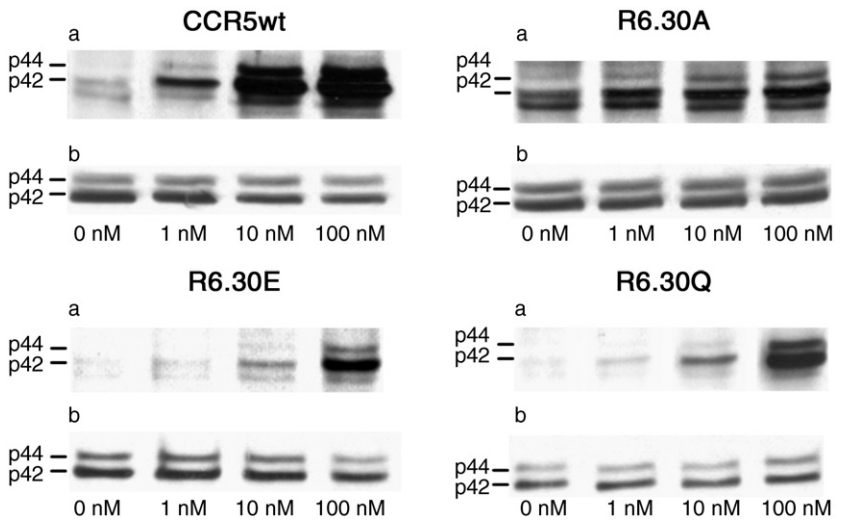

Fig. 7. MAP kinase activation by CCR5 mutants. Immunoblot detection of phosphorylated p42/p44 MAP kinases revealed with anti-phospho p42/p44. CHO-K1 cells expressing either wt or mutant CCR5 were stimulated with MIP-1β at three different concentrations (1, 10, and 100 nM) (upper panel). Detection of total p42/p44 by Western blotting was used to ascertain that an equal amount of material was loaded in each lane (lower panel). A typical experiment out of three performed independently is shown.

R6.30Q and D2.40A mutants displayed expression levels similar to that of wild-type CCR5, whereas D2.40R showed decreased expression. The D2.40A/R6.30A and D2.40R/R6.30D double mutants were characterized by surface expression levels similar to that of their single 2.40 counterpart. Western blot analysis performed on crude lysates of cells expressing the mutant receptors showed that the amount of CCR5 immunodetected correlated well with cell surface expression measured by FACS, indicating that the mutations did not affect the subcellular partitioning of the receptor (data not shown).

3.3. Oligomerization of CCR5 mutants

We have previously reported BRET and binding data demonstrating that CCR5 homodimerize [12,15]. Before studying further the functional consequences of the mutations on receptor properties, we tested whether these mutations could influence CCR5 dimerization in living cells, by using the BRET technique. As described previously [15], energy transfer was detected between CCR5-h*R*Luc and CCR5-EYFP (Fig. 3) in an agonist-independent manner. Similarly, energy transfer was detected between the various mutants fused to h*R*luc and to EYFP (Fig. 3). Similar transfers of energy were obtained between CCR5 mutants fused to h*R*luc and *wt*CCR5-EYFP or between *wt*CCR5-h*R*luc and mutants fused to EYFP (Supplementary data). The parameters of energy transfer ($BRET_{50}$, $BRET_{MAX}$) were in the same range for dimers of wild-type and mutants receptors, confirming that the ability to form homodimers is not affected by the mutations analyzed here.

3.4. Constitutive activity of the mutant receptors

CCR5 was previously reported to display a constitutive activity, characterized by its ability to activate G proteins and intracellular cascades in an agonist-independent manner [7,51]. This constitutive activity is best demonstrated in a GTPγ^{35}S binding assay and is abrogated by TAK-779, a non-peptidic CCR5 ligand with inverse agonist properties. We determined the functional consequences of the mutations and their combination on the constitutive activity of CCR5 in a GTPγ^{35}S binding assay on membranes prepared from clones expressing similar levels of receptor (Fig. 4A). As previously reported, GTPγ^{35}S binding to wild-type CCR5-expressing membranes was partially inhibited in the presence of TAK-779. In subsequent analyses, the GTPγ^{35}S binding in the presence of TAK-779 was considered as the basal G protein activity, while the increment in the absence of TAK-779 was recorded as a measure of the receptor constitutive activity.

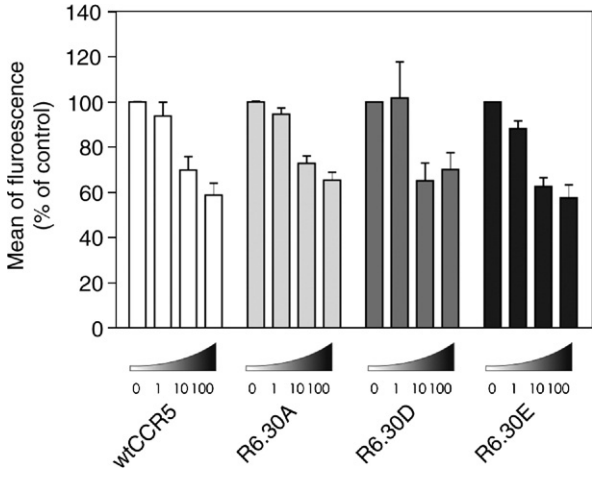

Fig. 8. Chemokine-induced internalization of CCR5 mutants. CHO-K1 cells expressing wild-type or mutant CCR5 were incubated with various concentrations of MIP-1β (nM) at 37 °C. Cell surface CCR5 was detected by flow cytometry using a saturating concentration of the 2D7-PE antibody. Results were normalized for the fluorescence of unstimulated cells (100%) and for background fluorescence (0%). All experiments were performed in duplicates (error bars represent S.E.M.).

Mutation of the charged residues at positions 6.30 and 2.40 reduced the constitutive activity although to a variable degree. R6.30A and D2.40A and D2.40R substitutions decreased the constitutive activity by about half. In contrast, the R6.30Q, R6.30D, R6.30E mutants were devoid of significant constitutive activity. In order to ascertain that this apparent lack of constitutive activity was not due to the inability of TAK-779 to bind the receptor, the affinity of the compound was tested for selected mutants in a competitive binding assay using MIP-1β as a tracer and TAK-779 was found to bind the mutant receptors with the same affinity as wild-type CCR5 (Fig. 4B). The combination of R6.30A and D2.40A mutations resulted in additive effects as compared to the individual mutations, while the combination of R6.30D and D2.40R mutations did not restore constitutive activity, suggesting that the two residues participate to distinct interaction networks. Finally, we observed that most of these mutants led, upon stimulation by RANTES, to a significant increase of GTPγ^{35}S binding (two- to four-fold the basal level), with the exception of the R6.30D, R6.30E and R6.30D/D2.40R mutants, for which the effect of the agonist was very weak.

3.5. Binding and functional properties of the mutant receptors

We next characterized the affinity of the mutant receptors for various CCR5 agonists (RANTES, MIP-1β, MIP-1α and MCP-2), by using ^{125}I-MIP-1β as labeled tracer and the four chemokines as competitors (Fig. 5 and Table 1). Replacement of the arginine at position 6.30 by an aspartate or a glutamate abolished detectable binding (data not shown), whereas the R6.30A or R6.30Q substitutions did not affect significantly chemokine binding to the receptor. The D2.40A and D2.40R mutants bound chemokines as efficiently as wild-type CCR5.

The mutants were further tested for their functional response in an aequorin-based calcium mobilization assay (Fig. 6 and Table 1). In line with the results of the binding experiments, the R6.30E and R6.30D mutants did not respond to chemokines in this assay, up to a concentration of 1 μM. The functional response of the R6.30A mutant was modestly impaired, while that of R6.30Q was strongly reduced. Finally, the D2.40A substitution did not affect signaling significantly, whereas the D2.40R mutation reduced the efficacy of chemokines by about one order of magnitude. Previous studies have shown that activation of CCR5 can also lead to the activation of p42/p44 MAP-kinases [52,53]. We therefore investigated the influence of selected CCR5 mutations on MAP-kinases activation. Stimulation of CCR5 by MIP-1β led to a dose-dependent activation of p42/p44. In this assay, MIP-1β stimulated the R6.30A or R6.30Q mutants although with a reduced efficiency as compared to wild-type CCR5. Unexpectedly, the R6.30E mutant, which did not respond in a calcium mobilization assay, and for which binding was undetectable, resulted in a significant activation of p42/p44 for the highest concentrations of MIP-1β (Fig. 7).

3.6. Down-regulation of the mutant receptors

As for other GPCRs, CCR5 desensitization, as a result of ligand stimulation, requires phosphorylation of the receptor C-terminus and recruitment of β-arrestin, which ultimately leads to clathrin-dependent internalization [54,55]. We thus investigated whether mutant CCR5 receptors were impaired in their chemokine-induced endocytosis behavior. Exposure to MIP-1β for 30 min resulted in a dose-dependent decrease of cell surface expression of wild-type CCR5. The R6.30A mutant behaved similarly, which was not unexpected given the relatively mild alteration of its binding and activation profile in other assays. Interestingly, internalization of the R6.30D and R6.30E mutants following MIP-1β stimulation was similar to that detected for wild-type CCR5, despite their low affinity for chemokine ligands (Fig. 8).

4. Discussion

On the basis of studies performed on various receptors, the mechanism governing activation of rhodopsin-like G protein-coupled receptors was proposed to involve a relative movement of TM3 and TM6. According to a currently accepted model, the cytoplasmic end of TM6 would, upon activation, move away from TM3, while rotating on its axis [23,25] and the side chain of residue R3.50 would shift out of a polar pocket formed by D/E3.49 and D/E6.30 in the resting state [19,20,56]. The so-called DRY lock model is supported by studies showing that mutations of D/E3.49 or D/E6.30 neutralizing the side chains lead to constitutive activity of receptors [19,25,27–29]. However, this model was validated only for receptors sharing a negatively charged residue at position 6.30, and about 30% of GPCRs, including chemokine receptors, display a positively charged residue at that position. We therefore questioned how to apply the DRY lock model to such receptors. Using CCR5 as a model, we investigated the role of positively charged amino-acids at position 6.30 on the functional properties of GPCRs. To our knowledge, this is the first study investigating such role in an attempt to extend the DRY lock model to GPCRs that do not share the key residues involved.

4.1. Functional role of R6.30 in CCR5 receptor

Before studying the functional consequences of the mutations affecting R6.30, we tested the cell surface localization and dimerization properties of the CCR5 mutants and showed that all mutants were expressed at the cell surface (although at reduced levels for some) and dimerized as efficiently as wild-type CCR5. By using a GTPγ^{35}S binding assay, we showed that CCR5 displayed a significant constitutive activity, i.e. an activity in the absence of agonist, which can be abrogated by the inverse agonist TAK-779, in agreement with our previous studies [7]. We show here that the level of constitutive activity of the mutants is modified according to the nature of the interaction allowed between R3.50 in TM3 and the side chain of residue 6.30 in TM6. In the wild-type receptor, position 6.30 is occupied by a positively charged residue (R6.30) that does not support interaction with R3.50, and would rather promote repulsion between TM3 and TM6. Neutralization of the residue (R6.30A) decreases the constitutive activity by half. Allowing an interaction by the introduction at position 6.30 of TM6 a

hydrogen bonding amino-acid (R6.30Q) or an acidic residue (R6.30D or E) results in a decrease of constitutive activity, down to undetectable levels. This observation in CCR5 is therefore reminiscent of situations described for D/E6.30-containing receptors, in which the mutation of position 6.30 promoted constitutive activity. Despite the absence of a classical DRY lock in CCR5, the overall structure of the receptor allows such lock to take place when the appropriate side chains are introduced, and as in other receptors, a correlation exists between the opening of the cytoplasmic face of the receptor and the interaction with the G protein [19,25–28,57]. However, in contrast to other receptors, R6.30 does not appear to contribute to maintaining the inactive state of CCR5, and other intracellular constrains maintaining its inactive state need to be considered. The recent finding that the D3.49N mutation, affecting the residue adjacent to R3.50, results in a decrease of CCR5 constitutive activity, rather than an increase as observed in D/E6.30-containing receptors, supports this hypothesis [7].

We showed also that mutations R6.30D and R6.30E, introducing in CCR5 the negative charge present in D/E6.30-containing receptors, abolished the high affinity chemokine binding, and most of the functional responses to chemokines. The inability of chemokines to activate the receptor in most assays, and the absence of detectable high-affinity binding site can also be attributed to the restoration of an ionic lock between D/E6.30 and R3.50. In the presence of D/E6.30, the inactive state is locked in such a way that agonist binding cannot trigger the conformational change to the active conformation (or very inefficiently), and only low affinity binding occurs. For CCR5, such low affinity site cannot be detected provided the expression level and the nonspecific binding of chemokines to proteoglycans. Similar results were observed for the μ opioid receptor that contains a leucine at position 6.30. Replacement of this leucine with a lysine increased the affinity of the receptor for its ligand, while its replacement by glutamate decreased significantly its affinity [45]. Interestingly, G protein-coupling is required for high affinity binding to these two receptors [16,58]. G protein interaction likely stabilizes the active conformation of the receptor, following the movement of TM6 away from TM3. G protein uncoupling or increasing the interaction between TM3 and TM6 therefore prevent the formation of a high affinity binding site, while repulsion between the two helices would favor the transition.

Interestingly, we observed that the R6.30D/E mutants, while unable to bind MIP-1β with high affinity and to signal in a calcium mobilization assay, were still able to stimulate MAP-kinases, and displayed internalization in response to MIP-1β. Inactive forms of other GPCRs were also shown to internalize as efficiently as their wild-type counterpart [59,60]. It was also reported that some receptor mutants bind efficiently their ligands without any subsequent internalization [61]. Our observations therefore support further the previous concept following which a receptor can adopt a range of active conformations, each linked to a set of downstream events, and that various signaling and internalization processes can be dissociated either by specific mutations, or according to the agonist used to activate the receptor.

CCR5 contains the known signatures distinctive of the rhodopsin family of GPCRs (the DRY, WxP(F/Y), and NPxxY motifs), involved in the process of receptor activation. However, the absence of the ionic lock between TM3 and TM6 in CCR5 due to R6.30 probably induces TM6 to adopt a less distorted Pro-kink α-helix. Fig. 1C shows the result of superimposing a more standard Pro-kink conformation (shown as a cylinder) to the highly conserved signatures in TM6, the backbones of the WxP(F/Y) motif and residue 6.40 engaged in the hydrogen bond with N7.49 of the NPxxY motif (see Results).

4.2. Functional role of D2.40 in CCR5

We showed also in this study that the D2.40A and D2.40R mutants display a reduced constitutive activity compared to wild-type CCR5. The functional consequences of mutations affecting D2.40 and R6.30 were essentially additives suggesting that these two residues participate to independent interaction networks. Nevertheless, mutation of D2.40 affects the receptor's function, and this residue appears therefore as involved in the CCR5 activation mechanism. In class A (rhodopsin-like) GPCRs, position 2.40 is occupied by either Asn (40%), Asp (10%), Phe, Tyr, or His (16%), Ser or Thr (14%), Lys or Arg (4%), or other amino acids (16%) [46]. The N2.40A mutation in rhodopsin results in decreased G_t-dependent activation by approximately 27% [62], while the R2.40H substitution in the TSH receptor decreases TSH-dependent cAMP response [63]. Thus, in these two other receptors, residue 2.40 also appears important in stabilizing the active state of the receptor.

5. Conclusion

Taken together, our data support the concept that CCR5 shares a common structure with rhodopsin and other receptors for which the DRY lock was proposed. This means that the intracellular parts of TM3 and TM6 interact in the resting state and separate upon activation of the receptor. However, position 6.30 does not contribute to maintaining the inactive state of the receptor through an ionic interaction with R3.50, but rather favors the active state. Neutralization of this residue results in a decreased constitutive activity while introduction of a negative charge generates a receptor that has lost most of its signaling properties and its ability to bind chemokines with high affinity. It appears therefore that the inactive state of GPCRs is maintained by a complex network of interactions between transmembrane helices. For some receptors, the DRY lock seems to play an important role within this network, in others the side chains involved in the DRY lock are not present, and other interactions are expected to play a similar role. Restoring an operational DRY lock in these receptors favors greatly the inactive state, in such a way that agonists are now unable to promote efficiently the conformational change. Finally, our data bring further support to the existence of multiple active states of GPCRs, each being able to trigger a distinct set of downstream events.

Acknowledgements

This work was supported by the Actions de Recherche Concertées of the Communauté Française de Belgique, the French Agence Nationale de Recherche sur le SIDA, the Belgian programme on Interuniversity Poles of attraction initiated by the Belgian State, Prime Minister's Office, Science Policy Programming, the European Union (grants LSHB-CT-2003-503337/GPCRs and LSHB-CT-2005-518167/INNO-CHEM), the Fonds de la Recherche Scientifique Médicale of Belgium, and the Fondation Médicale Reine Elisabeth. The scientific responsibility is assumed by the authors. CdP is supported by a fellowship of the Fonds d'encouragement à la Recherche dans l'Industrie et l'Agriculture (FRIA).

Appendix A. Supplementary data

Supplementary data associated with this article can be found, in the online version, at doi:10.1016/j.cellsig.2007.01.022.

References

[1] J.M.R. Frade, M. Llorente, M. Mellado, J. Alcami, J.C. Gutierrez-Ramos, A. Zaballos, G. del Real, C. Martinez-A, Journal of Clinical Investigation 100 (1997) 497.
[2] R.L. Rabin, M.K. Park, F. Liao, R. Swofford, D. Stephany, J.M. Farber, Journal of Immunology 162 (1999) 3840.
[3] P.M. Murphy, M. Baggiolini, I.F. Charo, C.A. Hebert, R. Horuk, K. Matsushima, L.H. Miller, J.J. Oppenheim, C.A. Power, Pharmacological Reviews 52 (2000) 145.
[4] M. Samson, F. Libert, B.J. Doranz, J. Rucker, C. Liesnard, C.M. Farber, S. Saragosti, C. Lapoumeroulie, J. Cognaux, C. Forceille, G. Muyldermans, C. Verhofstede, G. Burtonboy, M. Georges, T. Imai, S. Rana, Y. Yi, R.J. Smyth, R.G. Collman, R.W. Doms, G. Vassart, M. Parmentier, Nature 382 (1996) 722.
[5] C. Blanpain, B.J. Doranz, J. Vakili, J. Rucker, C. Govaerts, S.S. Baik, O. Lorthioir, I. Migeotte, F. Libert, F. Baleux, G. Vassart, R.W. Doms, M. Parmentier, Journal of Biological Chemistry 274 (1999) 34719.
[6] M. Detheux, L. Standker, J. Vakili, J. Munch, U. Forssmann, K. Adermann, S. Pohlmann, G. Vassart, F. Kirchhoff, M. Parmentier, W.G. Forssmann, Journal of Experimental Medicine 192 (2000) 1501.
[7] B. Lagane, S. Ballet, T. Planchenault, K. Balabanian, E. Le Poul, C. Blanpain, Y. Percherancier, I. Staropoli, G. Vassart, M. Oppermann, M. Parmentier, F. Bachelerie, Molecular Pharmacology 67 (2005) 1966.
[8] E.A. Berger, P.M. Murphy, J.M. Farber, Annual Review of Immunology 17 (1999) 657.
[9] C. Gerard, B.J. Rollins, Nature Immunology 2 (2001) 108.
[10] M. Benkirane, D.Y. Jin, R.F. Chun, R.A. Koup, K.T. Jeang, Journal of Biological Chemistry 272 (1997) 30603.
[11] M. Mellado, J.M. Rodriguez-Frade, A.J. Vila-Coro, S. Fernandez, d.A. Martin, D.R. Jones, J.L. Toran, A. Martinez, EMBO Journal 20 (2001) 2497.
[12] H. Issafras, S. Angers, S. Bulenger, C. Blanpain, M. Parmentier, C. Labbe-Jullie, M. Bouvier, S. Marullo, Journal of Biological Chemistry 277 (2002) 34666.
[13] P. Hernanz-Falcon, J.M. Rodriguez-Frade, A. Serrano, D. Juan, A. del Sol, S.F. Soriano, F. Roncal, L. Gomez, A. Valencia, A. Martinez, M. Mellado, Nature Immunology 5 (2004) 216.
[14] Y. Percherancier, Y.A. Berchiche, I. Slight, R. Volkmer-Engert, H. Tamamura, N. Fujii, M. Bouvier, N. Heveker, Journal of Biological Chemistry 280 (2005) 9895.
[15] L. El Asmar, J.Y. Springael, S. Ballet, E.U. Andrieu, G. Vassart, M. Parmentier, Molecular Pharmacology 67 (2005) 460.
[16] J.Y. Springael, P.N. Le Minh, E. Urizar, S. Costagliola, G. Vassart, M. Parmentier, Molecular Pharmacology 69 (2006) 1652.
[17] A. Jongejan, R. Leurs, Archiv der Pharmazie (Weinheim) 338 (2005) 248.
[18] C. Bissantz, Journal of Receptor and Signal Transduction Research 23 (2003) 123.
[19] J.A. Ballesteros, A.D. Jensen, G. Liapakis, S.G. Rasmussen, L. Shi, U. Gether, J.A. Javitch, Journal of Biological Chemistry 276 (2001) 29171.
[20] E. Urizar, S. Claeysen, X. Deupi, C. Govaerts, S. Costagliola, G. Vassart, L. Pardo, Journal of Biological Chemistry 280 (2005) 17135.
[21] A. Jongejan, M. Bruysters, J.A. Ballesteros, E. Haaksma, R.A. Bakker, L. Pardo, R. Leurs, Nature Chemical Biology 1 (2005) 98.
[22] L. Shi, G. Liapakis, R. Xu, F. Guarnieri, J.A. Ballesteros, J.A. Javitch, Journal of Biological Chemistry 277 (2002) 40989.
[23] D.L. Farrens, C. Altenbach, K. Yang, W.L. Hubbell, H.G. Khorana, Science 274 (1996) 768.
[24] J.A. Ballesteros, L. Shi, J.A. Javitch, Molecular Pharmacology 60 (2001) 1.
[25] U. Gether, Endocrine Reviews 21 (2000) 90.
[26] P.J. Greasley, F. Fanelli, O. Rossier, L. Abuin, S. Cotecchia, Molecular Pharmacology 61 (2002) 1025.
[27] M. Ascoli, F. Fanelli, D.L. Segaloff, Endocrine Reviews 23 (2002) 141.
[28] L. Montanelli, J.J. Van Durme, G. Smits, M. Bonomi, P. Rodien, E.J. Devor, K. Moffat-Wilson, L. Pardo, G. Vassart, S. Costagliola, Molecular Endocrinology 18 (2004) 2061.
[29] S. Claeysen, C. Govaerts, A. Lefort, J. Van Sande, S. Costagliola, L. Pardo, G. Vassart, FEBS Letters 517 (2002) 195.
[30] H.H. Ho, N. Ganeshalingam, A. Rosenhouse-Dantsker, R. Osman, M.C. Gershengorn, Journal of Biological Chemistry 276 (2001) 1376.
[31] J.A. Ballesteros, H. Weinstein, Methods Neurosciences 25 (1995) 366.
[32] M. Samson, G. LaRosa, F. Libert, P. Paindavoine, M. Detheux, G. Vassart, M. Parmentier, Journal of Biological Chemistry 272 (1997) 24934.
[33] E. Urizar, L. Montanelli, T. Loy, M. Bonomi, S. Swillens, C. Gales, M. Bouvier, G. Smits, G. Vassart, S. Costagliola, EMBO Journal 24 (2005) 1954.
[34] C. Govaerts, C. Blanpain, X. Deupi, S. Ballet, J.A. Ballesteros, S.J. Wodak, G. Vassart, L. Pardo, M. Parmentier, Journal of Biological Chemistry 276 (2001) 13217.
[35] C. Govaerts, A. Bondue, J.Y. Springael, M. Olivella, X. Deupi, E. Le Poul, S.J. Wodak, M. Parmentier, L. Pardo, C. Blanpain, Journal of Biological Chemistry 278 (2003) 1892.
[36] C. Govaerts, A. Lefort, S. Costagliola, S.J. Wodak, J.A. Ballesteros, J. Van Sande, L. Pardo, G. Vassart, Journal of Biological Chemistry 276 (2001) 22991.
[37] J. Li, P.C. Edwards, M. Burghammer, C. Villa, G.F.X. Schertler, Journal of Molecular Biology 343 (2004) 1409.
[38] M. Bansal, S. Kumar, R. Velavan, Journal of Biomolecular Structure & Dynamics 17 (2000) 811.
[39] I. Visiers, B.B. Braunheim, H. Weinstein, Protein Engineering 13 (2000) 603.
[40] J. Van Durme, F. Horn, S. Costagliola, G. Vriend, G. Vassart, Molecular Endocrinology 20 (2006) 2247.
[41] F.S. Cordes, J.N. Bright, M.S.P. Sansom, Journal of Molecular Biology 323 (2002) 951.
[42] X. Deupi, M. Olivella, C. Govaerts, J.A. Ballesteros, M. Campillo, L. Pardo, Biophysical Journal 86 (2004) 105.
[43] L. Pardo, X. Deupi, N. Dolker, M.L. Lopez-Rodriguez, M. Campillo, Journal of Computer-Aided Molecular Design (2006).
[44] J.J. Ruprecht, T. Mielke, R. Vogel, C. Villa, G.F.X. Schertler, EMBO Journal 23 (2004) 3609.
[45] P. Huang, I. Visiers, H. Weinstein, L.Y. Liu-Chen, Biochemistry 41 (2002) 11972.
[46] T. Mirzadegan, G. Benko, S. Filipek, K. Palczewski, Biochemistry 42 (2003) 2759.
[47] T. Mirzadegan, F. Diehl, B. Ebi, S. Bhakta, I. Polsky, D. McCarley, M. Mulkins, G.S. Weatherhead, J.M. Lapierre, J. Dankwardt, D. Morgans Jr., R. Wilhelm, K. Jarnagin, Journal of Biological Chemistry 275 (2000) 25562.
[48] T. Okada, Y. Fujiyoshi, M. Silow, J. Navarro, E.M. Landau, Y. Shichida, Proceedings of the National Academy of Sciences of the United States of America 99 (2002) 5982.
[49] O. Fritze, S. Filipek, V. Kuksa, K. Palczewski, K.P. Hofmann, O.P. Ernst, Proceedings of the National Academy of Sciences of the United States of America 100 (2003) 2290.

[50] C. Prioleau, I. Visiers, B.J. Ebersole, H. Weinstein, S.C. Sealfon, Journal of Biological Chemistry 277 (2002) 36577.
[51] T. Dragic, A. Trkola, D.A. Thompson, E.G. Cormier, F.A. Kajumo, E. Maxwell, S.W. Lin, W. Ying, S.O. Smith, T.P. Sakmar, J.P. Moore, Proceedings of the National Academy of Sciences of the United States of America 97 (2000) 5639.
[52] D.J. Dairaghi, K. Franz-Bacon, E. Callas, J. Cupp, T.J. Schall, S.A. Tamraz, S.A. Boehme, N. Taylor, K.B. Bacon, Blood 91 (1998) 2905.
[53] D. Misse, P.O. Esteve, B. Renneboog, M. Vidal, M. Cerutti, Y. St Pierre, H. Yssel, M. Parmentier, F. Veas, Blood 98 (2001) 541.
[54] K. Kraft, H. Olbrich, I. Majoul, M. Mack, A. Proudfoot, M. Oppermann, Journal of Biological Chemistry 276 (2001) 34408.
[55] A. Mueller, E. Kelly, P.G. Strange, Blood 99 (2002) 785.
[56] A. Scheer, F. Fanelli, T. Costa, P.G. De Benedetti, S. Cotecchia, EMBO Journal 15 (1996) 3566.
[57] U. Ringkananont, J. Van Durme, L. Montanelli, F. Ugrasbul, Y.M. Yu, R.E. Weiss, S. Refetoff, H. Grasberger, Molecular Endocrinology 20 (2006) 893.
[58] R. Staudinger, X. Wang, J.C. Bandres, Biochemical and Biophysical Research Communications 286 (2001) 41.
[59] A.H. Cheung, R.A. Dixon, W.S. Hill, I.S. Sigal, C.D. Strader, Molecular Pharmacology 37 (1990) 775.
[60] L. Hunyady, A.J. Baukal, T. Balla, K.J. Catt, Journal of Biological Chemistry 269 (1994) 24798.
[61] D.E. Keith, S.R. Murray, P.A. Zaki, P.C. Chu, D.V. Lissin, L. Kang, C.J. Evans, M. von Zastrow, Journal of Biological Chemistry 271 (1996) 19021.
[62] L. Shi, Z. Shi, J. Zhang, Q. Ma, D. Kong, L. Yang, Y. Tan, Chinese Medical Sciences Journal 10 (1995) 30.
[63] T. Nagashima, M. Murakami, K. Onigata, T. Morimura, K. Nagashima, M. Mori, A. Morikawa, Thyroid 11 (2001) 551.